journal

J. Am. Ceram. Soc., **88** [9] 2456–2460 (2005)
DOI: 10.1111/j.1551-2916.2005.00441.x
© 2005 The American Ceramic Society

Surface Chemical and Leakage Current Density Characteristics of Nanocrystalline Ag–$Ba_{0.5}Sr_{0.5}TiO_3$ Thin Films

Kampurath P. Jayadevan, Chi-Yi Liu, and Tseung-Yuen Tseng†

Department of Electronics Engineering and Institute of Electronics, National Chiao-Tung University, Hsinchu 300, Taiwan

Nanocrystalline xAg–$(1-x)Ba_{0.5}Sr_{0.5}TiO_3$ (Ag–BST, $0 \le x \le 0.1$, where x is the mole fraction of Ag) thin films have been deposited on Pt/Ti/SiO_2/Si substrates by a sol–gel method. The films have been characterized by X-ray diffraction (XRD), scanning electron microscopy, and X-ray photoelectron spectroscopy (XPS). The core-level XPS of oxygen (O1*s*) of the Ag–BST films indicate that an optimum amount of Ag ($x = 0.02$ or 2 mol%) enhances the binding energy of oxygen, possibly through a mechanism in which the electrophilic oxygen dissociates from the Ag surface and fills the oxygen vacancies. Similarly, the binding energy of Ag (Ag3*d*) shows a shift toward a higher value with increasing Ag up to 4 mol%, probably because of the chemical shift of Ag in BST along the surface layers, surface relaxation, or changes in the Fermi level of small Ag particles in the solid solution range of Ag in BST films ($x \le 0.04$). The leakage current density of 2 mol% Ag-added BST ($\sim 10^{-6}$ A/cm^2) is less by about an order of magnitude than pure BST at an electric field of 200 kV/cm. A defect model is proposed to explain the observed leakage current density of Ag–BST films satisfactorily.

I. Introduction

THE high-permittivity (Ba,Sr)TiO_3 (BST) thin films have been intensively studied in recent years as a potential dielectric material for the development of capacitors in microwave devices and future ultra high-density dynamic random access memories (DRAM) because of their low dielectric loss, high breakdown field strength, tunable dielectric constant, low leakage current density, and high reliability.[1] The present research interests in this class of high-permittivity perovskite oxides are directed toward achieving improved performance of miniaturized BST capacitors by tuning the processing parameters,[2] reducing the leakage current density by suitable dopants,[3] fabricating composite or multilayer capacitors and superlattices with enhanced properties,[4] and adopting innovative procedures for the integration of high-permittivity films directly on silicon (Si).[5] Among the various factors that lead to high leakage current density in BST thin films, oxygen vacancy formation at the film/electrode interface has been identified as a major cause for current conduction and performance degradation of BST capacitors.[6,7] Deposition or annealing of BST films at selected partial pressures of oxygen has been adopted as a suitable method to reduce the oxygen vacancies, which are omnipresent in an equilibrium perovskite structure, as demonstrated by Tsai *et al.*[6] for the sputter-deposited $Ba_{0.5}Sr_{0.5}TiO_3$ (BST) thin films at various oxygen mixing ratios with argon (O_2/Ar+O_2). Our present investigation into the silver (Ag)–BST system has been motivated by a recent study by Srivastava *et al.*,[8] which indicates a significant reduction in leakage current density of pulse-laser deposited (Ba,Sr)TiO_3 thin films that are prepared from a BST target with 5 wt% Ag. The proposed explanation for the reduction in leakage current can be summarized as follows: the unstable silver oxides (Ag_xO) that are formed during the film deposition and annealing decompose to Ag, which remains intact with a low drive for oxidation[9] in the BST under ambient conditions. The irreversible decomposition of Ag_xO[10] would compensate oxygen vacancies; thereby, a less defective BST would form along with a reduction in leakage current.[8] However, an experimental study to verify this mechanism has not been reported so far. In order to obtain a possible experimental evidence for the oxygenation of BST films in the presence of Ag, we have carried out an X-ray photoelectron spectroscopic (XPS) investigation of sol–gel-derived nanocrystalline Ag–BST thin films. An optimum amount of Ag (2 mol%) is found to enhance the binding energy of surface oxygen and the O1*s* peak intensity. This observation is further supported by the leakage current density characteristics that show a reduction at an electric field higher than 150 kV/cm for 1 and 2 mol% Ag when compared with pure BST. The grain size and phase have been characterized by X-ray diffraction (XRD), while scanning electron microscopic (SEM) investigation of the surface of the Ag–BST films provides morphology characteristics. Sol–gel processing is undoubtedly one of the easiest methods for the deposition of thin films with excellent control over the composition of the reactive components in solution.[4] It can also be used as an economically affordable pilot-scale technique for the fabrication of novel solid solutions or composites. The nanocrystalline Ag–BST thin films have been prepared by an acetate–precursor sol–gel route.[11] The method has been chosen because of its relatively simple approach for obtaining a clear and homogeneous solution for deposition.

II. Experimental Procedure

The scheme for the preparation of the precursor solutions for xAg–$(1-x)Ba_{0.5}Sr_{0.5}TiO_3$ (Ag–BST), where x is the mole fraction of Ag in the BST thin films, is summarized as follows: the Ag contents in the Ag–BST thin films were selected as $x = 0.01$, 0.02, 0.03, 0.04, and 0.1 (1, 2, 3, 4, and 10 mol%), with the corresponding variations in the BST precursor as 0.99, 0.98, 0.97, 0.96, and 0.90. For convenience, the composition of the films would be presented henceforth as Ag(X)–BST, where X refers to the mol% of Ag in BST films. The stoichiometric amounts of the reactants, $Ba(OAc)_2$, $Sr(OAc)_2$, Ti(*i*-OPr)$_4$, and Ag(OAc) (OAc acetate and *i*-OPr isopropoxide), were dissolved in 25 mL acetic acid at about 90°C. The solution was stabilized by the addition of ~8.5 mL ethylene glycol so as to maintain the ratio of acetic acid to ethylene glycol as 3:1, which would lead to a uniform microstructure as reported by Tahan *et al.*[11] The clear and homogeneous solutions (0.15 M) obtained after 60 min of stirring were kept at room temperature and aged for about 12–24 h before spin coating. An undoped BST precursor solution was prepared to deposit the reference BST film. The solutions were filtered using a syringe attached with a 0.2 μm filter onto

I. W. Chen—contributing editor

Manuscript No. 20260. Received August 20, 2004; approved March 5, 2005.
This work was supported by the National Science Council (NSC) of Republic of China under the Project No. NSC 92-2215-E009-016.
†Author to whom correspondence should be addressed. e-mail: tseng@cc.nctu.edu.tw

Pt (100 nm)/Ti (5 nm)/SiO_2 (500 nm)/Si substrates and then spin coated in two steps (1000 rpm for 15 s and 4000 rpm for 60 s). The coated layers were dried at 200°C for 10 min and then pyrolyzed at 500°C for 30 min. The coating and pyrolysis steps were repeated 11 times to obtain ~210 nm thickness for each composition. The composition of Ag–BST films has not been modulated by the graded layer deposition technique in this study. During the deposition of each layer, a small portion of the substrate was masked so as to preserve the bottom Pt layer as an electrode for measurements. The films were finally annealed at 700°C for 2 h. The annealed films were characterized for phase formation and grain size using XRD (Rigaku D-Max/IIB X-ray Diffractometer, Rigaku, Japan, Cu$K\alpha$ $\lambda = 0.15405$ nm, 0.02° 2θ step). The microstructure and cross-section of the films were examined using a SEM (Hitachi S4700, Hitachi, Japan). XPS were recorded under ultra high-vacuum conditions using a VG Microlab 310F spectrometer (VG Scientific UK) with Al$K\alpha$ radiation of 1486.6 eV energy. For electrical measurements of the films, metal–insulator–metal (MIM) structures were fabricated by depositing 100 nm thick Pt top electrodes with a diameter of 250 μm by electron beam evaporation through a shadow mask. The current–voltage (I–V) characteristics were recorded by using an Agilent 4155C semiconductor parameter analyzer (Agilent Technologies, Japan) under bias voltage in the range from −5 to 5 V.

III. Results and Discussion

(1) Phase, Crystallinity, and Grain Size

The spin coated and thermally processed Ag–BST thin films on Pt/Ti/SiO_2/Si substrates were subjected to phase characterization and crystallite size determination using XRD. Figure 1 depicts the XRD patterns of the prepared films with Ag content up to 4 mol%. All the peaks are indexed to the BST phase, with no appearance of a second phase in the sample. The sharp (110) and (200) peaks of BST phase indicate that the films have good crystallinity, with the average grain size (t_{XRD}) varying from ~19 nm for Ag(2)–BST (the number in brackets refers to mol% of Ag in BST according to the scheme described under the experimental section) to ~25 nm for Ag(4)–BST as determined by using the Scherrer equation

$$t_{XRD} = 0.9\lambda/\beta \cos \theta_B \quad (1)$$

where λ is the wavelength of the Cu$K\alpha$ radiation, β is the full-width at half-maximum, (FWHM) and θ_B is the diffraction angle. The amounts of Ag added in the present study do not seem to suppress the average BST crystallite size. No significant variations in peak positions are detected as the Ag content is increased up to 4 mol%.

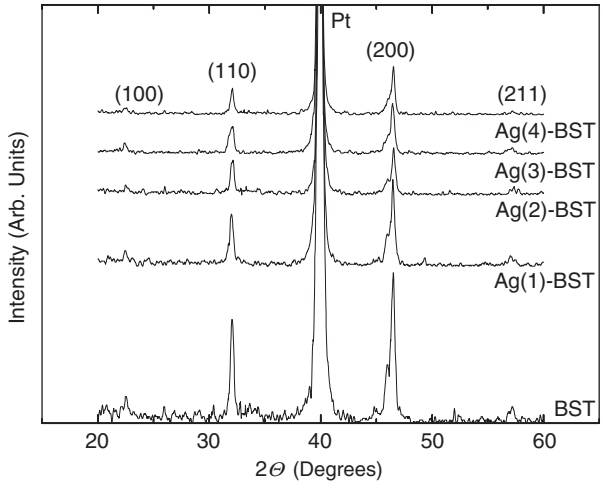

Fig. 1. X-ray diffraction (XRD) patterns of undoped BST, Ag(1)–BST, Ag(2)–BST, Ag(3)—BST, and Ag(4)–BST films crystallized at 700°C on Pt/Ti/SiO_2/Si substrates. The number in brackets refers to mol% of Ag.

(2) Surface Morphology

The microstructures of the prepared nanocrystalline Ag–BST films have been examined by SEM. Surface morphology characteristics of a selected set of films, undoped BST, Ag(2)–BST, and Ag(4)–BST, and cross-sectional SEM picture for Ag(2)–BST are shown in Fig. 2. Upon 2 mol% addition of Ag, significant modification of the microstructure is observed with the realization of a highly dense and uniform microstructure of an Ag(2)–BST film (Fig. 2(b)) in comparison with undoped BST (Fig. 2(a)). The average grain or agglomerate diameter (d_{SEM}) of Ag(2)–BST film is ~25 nm, which is comparable with the grain size obtained from the XRD analysis. The improvement of microstructure of Ag(2)–BST as compared with undoped BST could have been caused by the increased presence of Ag along the grain boundaries[8] close to the surface layers that lead to the formation of dense layers for the Ag(2)–BST film annealed at 700°C. The possibility of a significant reduction in the actual melting point of Ag (~960°C)[9] in the nanometer regime or an increase in the mobility of Ag in the shallow potential wells along the grain boundaries in the layers close to the surface might cause a quasi-melting[12] of the small Ag particles, as the direction of diffusion of Ag is toward the surface. The analysis of binding energy of Ag at the surface will be discussed in the next section and based on the leakage current density characteristics of Ag–BST films, a possible microstructure for the Ag–BST film will be proposed. The large island-like agglomerate formation in Ag(4)–BST (Fig. 2(c)) with significantly high crystallinity could have been caused by the further enhancement of grain boundary diffusion, as the mobility of Ag increases along the grain boundaries close to the surface. The dense and fine-grained microstructure of Ag(2)–BST film is also illustrated as a cross-sectional SEM picture in Fig. 2(d). The average thickness of the film is 210 ± 10 nm, as obtained from the cross-sectional SEM analysis (Fig. 2(d)).

(3) Surface Chemical States of Ag and Oxygen (O)

XPS corresponding to oxygen (O1s) in Ag–BST nanocrystalline thin films up to 2 mol% Ag and silver (Ag3d) up to 10 mol% Ag are presented in Fig. 3(a) and (b), respectively. The binding energy of O1s corresponding to undoped BST is 528.2 eV, which is less than the reported values of oxygen that range between 529 and 531 eV in perovskite (Ba,Sr)TiO_3,[13–16] possibly because of oxygen deficiency in our samples. As the Ag content is increased, there is a systematic shift of O1s peaks to higher binding energy (529.6 eV) with increasing intensity up to 2 mol% Ag (Ag(2)–BST). An example that illustrates the evidence of oxygenation

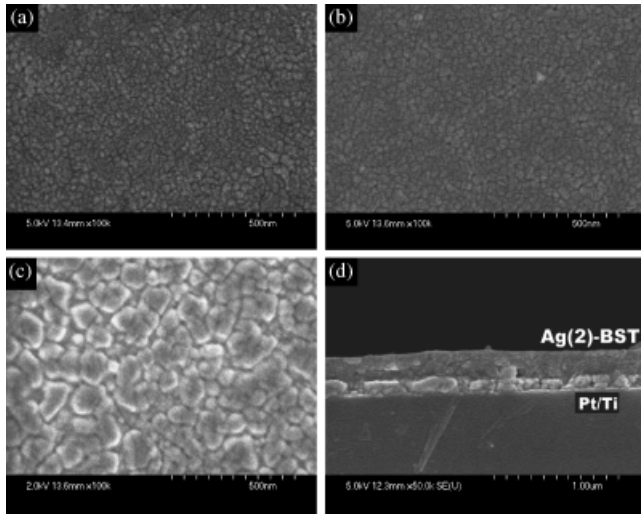

Fig. 2. Scanning electron micrographs (SEM) of the surface morphologies of (a) undoped BST (b) Ag(2)–BST, (c) Ag(4)–BST films, and (d) cross-section for ~210 nm thick Ag(2)–BST film to illustrate the dense microstructure. The scale bar for (a)–(c) is 500 nm and 1 μm for (d).

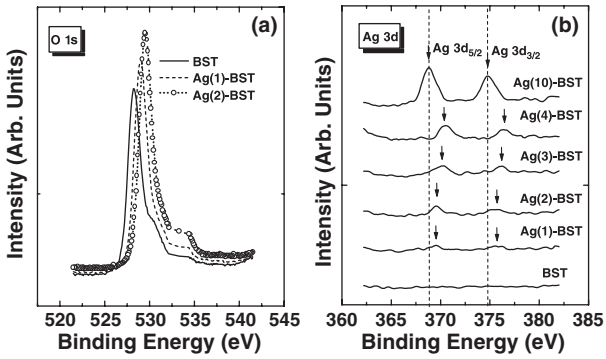

Fig. 3. X-ray photoelectron spectra (XPS) of (a) oxygen (O 1*s*), and (b) Ag3*d* for the films indicated in the figure.

from the XPS analysis is the shift of the O1*s* profile toward higher binding energy with an increase in the intensity that is observed for the Si substrate because of the incorporation of oxygen as the substrate is heated.[17] In our study, the enhancement of O1*s* signal of BST could have been caused by a catalytic oxidation in the presence of Ag. The reactivity of oxygen at the surface of Ag has been a topic of immense interest for the exploitation of Ag in catalysis, for the oxidation of organic molecules and removal of toxic gases from the environment.[18–23] The potential for catalytic oxygenation depends on the nature of the oxygen that is adsorbed on the Ag surface. The selective oxygenation of organic molecules using Ag as a catalyst implies that the oxygen adsorbed on the surface of Ag would be electrophilic, covalent, and weakly polarized.[18] When Ag is formed as a solid solution with BST, the electrophilic oxygen adsorbed on the surface of Ag would find a potentially stable site for occupancy, probably driven by the electrostatic potential in association with titanium ion (Ti^{4+})[24] in the BST. The observation that the O1*s* peaks in BST, Ag(1)–BST, and Ag(2)–BST do not show any splitting or distinct higher energy peak[25] and the comparable FWHM of O1*s* peaks (1.7–1.8 eV) indicate the oxygen species as O^{2-} ion in the BST or Ag–BST films. Therefore, the shift in the O1*s* peak and the increase in the intensity could have been caused by the filling of the oxygen vacancies, which is similar to the XPS study of the oxygenation of an oxygen-deficient MgO surface as reported by Peterka *et al.*[26] The increase in the oxygen content with increasing Ag in BST can be estimated from the XPS data and the value is an ~2 at.% increase in oxygen for Ag(2)–BST in comparison with pure BST. As the Ag content is increased to 4 mol%, the maximum binding energy value remains on the average in the shifted range. However, some irregularity of peak position in the binding energy curve has been observed beyond 2 mol% Ag (not shown here), which could probably be because of the onset of many competitive surface reactions such as Ag–Ag and Ag–BST interactions or changes in the electrostatic potential that depend on the coordination surrounding the titanium ion (Ti^{4+})[24] in the BST. A detailed surface analysis of the Ag–BST films would help to delineate the various competitive interactions at the Ag–BST surface.

As the O1*s* peaks do not show any splitting and exhibit only a single maximum with increasing Ag in BST, we conclude that there is no silver oxide formation in the film. The absence of silver oxides is further confirmed by the Ag3*d* spectra, which will be discussed later in this section. The broad hump with a low relative intensity at a higher binding energy of O1*s* may be because of the oxygen that binds to carbonaceous impurities[13,14] as this is observed in all samples including undoped BST. The enhanced oxygen binding energy in Ag–BST films could be related to the decomposition of unstable silver oxides[9] or short-lived transient compounds ($[Ag..O]^*$, oxygen chemisorbed on the surface of Ag)[27] well below the annealing temperature (700°C) of the BST films. In our study, the $[Ag..O]^*$ species (weakly adsorbed electrophilic oxygen species) are more likely to be present, as the deposition is not carried out in the presence of energetic oxygen species in a plasma (e.g., oxidation of an Ag foil to Ag_2O in an oxygen microwave plasma[28] or pulsed laser ablation of an Ag–BST target in an oxygen atmosphere[8]). The $[Ag..O]^*$ that is formed from the Ag precursor in the film would decompose according to the reaction

$$[Ag..O]^*(s) \rightarrow Ag_{Ag}(s) + 1/2O_2(g) \quad (2)$$

The filling of the oxygen vacancies can be written according to the Kröger–Vink notation as

$$1/2\,O_2(g) + V_O^{\bullet\bullet} + 2e' = O_O^x \quad (3)$$

As the sticking coefficient of oxygen on Ag surface is low,[27] and the favorable energetic path is filling of oxygen vacancies, the dissociated oxygen from $[Ag..O]^*$ (weakly electrophilic oxygen on Ag) may be involved in a surface chemical binding in BST films, which is manifested as a chemical shift in the O1*s* XPS spectrum as described earlier. The estimation of an increase in oxygen by about 2 at.% for Ag(2)–BST film when compared with pure BST indicates the possibility of reactions (2) and (3).

The evidence for Ag at the surface is derived from Ag3$d_{5/2}$ (BE ~ 369.5–370.5 eV) and Ag3$d_{3/2}$ (BE ~ 375.5–376.5 eV) levels of Ag3*d* XPS spectra (Fig. 3(b)) of Ag–BST films that have binding energy values closer to those reported for pure Ag (3$d_{5/2}$ ~ 368 eV and 3$d_{3/2}$ ~ 374 eV),[29] but higher than those of Ag_2O (3$d_{5/2}$ ~ 367.6 eV and 3$d_{3/2}$ ~ 373.6 eV),[29] AgO (3$d_{5/2}$ ~ 367.4 eV), and Ag_2CO_3 (3$d_{5/2}$ ~ 367.6 eV).[27] The higher binding energy value of Ag in Ag–BST than in its pure form may be attributed to the difference in the chemical environment of Ag, the relaxation effect, or the Fermi level shift. The total shift in the binding energy (ΔE_B) can be expressed as

$$\Delta E_B = \Delta E_C + \Delta E_R + \Delta E_F \quad (4)$$

where ΔE_C is the shift in the binding energy because of the difference in the chemical configuration (chemical shift), ΔE_R is the shift because of the contribution from the relaxation, and ΔE_F is the Fermi level contribution to the total binding energy shift.[21]

The ΔE_C in Eq. (4) represents the change in the electrostatic potential between the initial state and the final state because of the chemical shift.[30] Although the solubility of Ag in stoichiometric BST-related bulk perovskite oxides is stated to be negligible,[31,32] the shifts of the Ag3*d* peaks in the XPS spectra to higher binding energy values as the Ag content is increased to 4 mol% Ag (Fig. 3(b)) indicate that along the surface layers of the Ag–BST film, a small amount of Ag could be soluble as the Ag radius would be comparable with (Ba,Sr)-site radius.[33] Therefore, the oxygen vacancy gets compensated through a Schottky equilibrium at the surface layers. The ΔE_C would be more pronounced when Ag is present in low concentration in the solid solution xAg–$(1-x)$$Ba_{0.5}Sr_{0.5}TiO_3$ ($x \leq 0.04$) because of the defective coordination environment close to the surface, difference in size between Ag and the $(Ba,Sr)^{2+}$ ions, and the reduced coulomb interaction of substituted Ag with the oxide ions. The XPS analysis that confirms the solid solubility of Ag in perovskite BST has not been reported in the literature, but that of the Ag-doped perovskite $LaCoO_3$ indicates that the neutral Ag exists at the surface of $LaCoO_3$ monoliths on catalyst support.[34] The study does not show any positive shift in the binding energy. The binding energy of Ag3*d* level shifts to that of Ag^+ ion, when the surface of the $LaCoO_3$ is etched to a depth of a few nanometers. The presence of Ag^+ ion in the bulk has been taken as the probable evidence for the A-site substitution in $LaCoO_3$. The Ag–BST system that we have investigated is nanocrystalline with the possibility of defective anionic sites at the surface that would promote the dissolution of Ag[35] along the surface layers of BST. Further detailed investigation of nanocrystalline thin films of Ag–BST would be required to understand the exact electronic state of Ag in BST.

From the XPS results of our study on Ag–BST films and those on Ag–$LaCoO_3$ in which neutral Ag has been identified at the surface,[34] it can be believed that the Ag diffuses toward the surface. The dense and uniform layer that we observe in the examination of surface morphology of Ag(2)–BST and large island-like agglomerates for Ag(4)–BST film in Figs. 2(b) and (c), respectively, could have been because of the presence of Ag, which has two roles when it diffuses to the surface layers: (1) modification of surface morphology of BST as derived from the SEM analysis and illustrated in Figs. 2 (b) and (c), and (2) dissolution of Ag in BST grains close to the surface as obtained from the XPS analysis (Fig. 3(b)).

The second term in Eq. (4), ΔE_R, is the relaxation energy that is required to excite a core-level electron to the valence state to neutralize the localized holes that are associated with the excited metallic atoms so that the translational symmetry of the infinite solid is preserved.[36] The contribution from ΔE_R will be negligible if there is pronounced screening effect from the valence electrons that helps to maintain the local charge neutrality. For very small particle sizes of Ag that are likely to be present in the Ag–BST films for low mole fractions of Ag ($x \leq 0.04$), the positively charged final state (excited state) would not be well screened and would therefore contribute to the shift of the binding energy in the form of relaxation energy (ΔE_R). For the BST film with 10 mol% Ag ($x = 0.1$), the shift toward binding energy that is lower than the samples with $x = 0.01$, 0.02, 0.03, and 0.04 indicates an increased Ag–Ag interaction and hence an improvement in screening.

In addition to ΔE_C and ΔE_R, there could also be a contribution from the ΔE_F in Eq. (4), as the original Fermi level of Ag could shift because of small particle sizes of Ag that is present in the Ag–BST solid solution. For low mole fractions or an optimum amount of Ag in BST ($x \leq 0.04$), the shift in the Fermi level of Ag would contribute to the ΔE_B, while undergoing an equilibration process with BST through space charge effect.[37] For the BST film with $x = 0.1$, the increased Ag–Ag interaction would reduce the contribution of ΔE_F to the ΔE_B. The three energy terms, ΔE_C, ΔE_R, and ΔE_F, would add to give a resultant shift in the Ag3*d* spectra (Fig. 3(b)). A detailed surface analysis would be required to quantify these effects and identify the exact mechanism in this system. From our XPS analysis, we suggest that the oxygenation and Schottky equilibration of oxygen vacancies are probably operative in Ag–BST films up to a small amount of Ag.

The absence of oxide phases of Ag is further confirmed by the Ag3*d* XPS spectrum of a 10 mol% Ag-added BST (Ag(10)–BST) (Fig. 3(b)). The spectrum indicates well-defined $3d_{5/2}$ and $3d_{3/2}$ peaks with the respective binding energy maxima of $\sim$368.8 and $\sim$374.7 eV that are close to those of pure Ag.[27,29] The shift toward binding energy value of pure Ag may be because of the increase in the Ag–Ag interaction that leads to the formation of Ag islands or clusters on the surface that form as a separate phase from BST. An additional evidence for the diffusion of Ag toward the surface could be derived from our capacitance–voltage (*C–V*) measurements of BST, Ag(1)–BST, and Ag(2)–BST films, which show an increasing asymmetry in the *C–V* curves with increasing Ag because of the surface modification of the Ag–BST films by Ag as reported in a recent letter.[38]

(4) Leakage Current Density Characteristics

The leakage current densities of MIM capacitors of configuration, Pt/Ag(0…4)–BST/Pt have been investigated and presented in Fig. 4. The asymmetry of the current density curves with higher leakage currents under reverse bias indicates the difference in the interface characteristics of the top and bottom electrodes with the film. The major contributing factor to the leakage current density of undoped BST films is believed to be because of the electrons associated with the oxygen vacancies. In the present study, we have observed a reproducible reduction in leakage current density by about an order of magnitude for the Ag(2)–BST-based MIM capacitor ($\sim 10^{-6}$ A/cm^2) at a high electric field of 200 kV/cm when measured under either biases in comparison with undoped BST ($\sim 10^{-5}$ A/cm^2). The dominant mechanism in Ag(1)–BST and Ag(2)–BST films might be steps (2) and (3) as indicated before. According to expression (3), it can be concluded that electrons are consumed during the oxygenation of the Ag(1 and 2)–BST films, which makes the film relatively *p*-type[39] compared with pure BST up to an optimum Ag content. The lowest leakage current density at 200 kV/cm is obtained for an Ag(2)–BST film, where a number of mechanisms may be working in concert so that an effective reduction in leakage current is obtained.

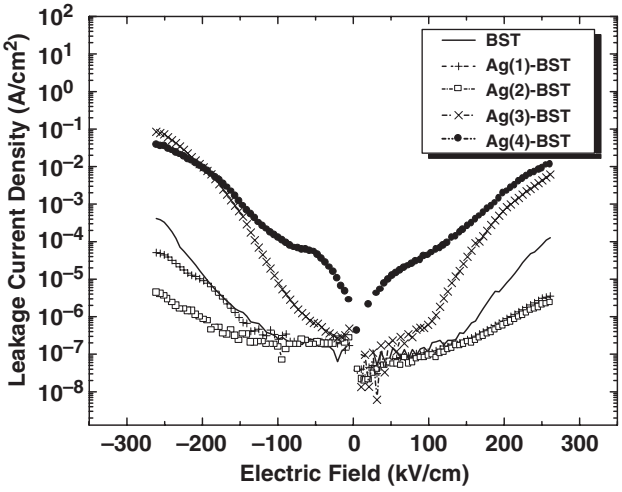

Fig. 4. Leakage current density characteristics of metal–insulator–metal (MIM) capacitors of configuration, Pt/Ag(0…4)–BST/Pt under forward and reverse biases.

The observed leakage current for a BST-based capacitor comprises the contributions from the electronic conduction and polarization loss.[6] As observed and discussed in our previous communication on dielectric characteristics of Ag(1)–BST and Ag(2)–BST,[38] there is a significant reduction in dielectric constant of Ag(2)–BST as compared with undoped BST, with the lowest dielectric loss tangent in the entire range of electric field measured. The observed reduction in loss factor has been ascribed to the dense microstructure, enhanced polarization pinning, and a series configuration of low-dielectric interface layers or metal–ceramic configuration of Ag and BST.[38] From this result, we conclude that the polarization loss is minimum for an Ag(2)–BST film. Moreover, as explained with the help of Eqs. (2) and (3), filling of oxygen vacancies may be predominant up to a certain amount of Ag. Upon increasing the Ag content to 3 mol%, the leakage current density increases rapidly beyond 100 kV/cm because of an increase in the concentration of electrons that results in increased electronic conductivity. The gradual increase in the electronic conduction with an increase in Ag is obvious as the current density curve rises with a higher slope at the beginning of the measurement at a low electric field as obtained in the case of Ag(4)–BST. Therefore, we conclude that a low leakage current is maintained only up to a certain amount of Ag in BST for which a series metal–ceramic configuration exists and oxygenation is dominant. In our samples, this series configuration is disrupted as the Ag content is increased to 3 mol% and beyond.

IV. Conclusions

In summary, an optimum amount of Ag (1 and 2 mol%) enhances the binding energy of surface oxygen and reduces the leakage current density of chemical solution-deposited Ag–BST nanocrystalline thin-film capacitors through a combination of a microstructure that maintains a series metal–ceramic configura-

tion for which the polarization loss is less and the filling of oxygen vacancy is dominant. In addition, there is also a slight enhancement of binding energy of Ag up to 4 mol% because of its possible chemical shift or dissolution along the surface layers of BST, surface relaxation effects, and Fermi-level shifts of Ag in the Ag–BST films. The leakage current increases and becomes higher than pure BST for Ag content greater than or equal to 3 mol% because of increased electronic conduction.

References

[1]M. Nayak, S. Ezhilvalavan, and T. Y. Tseng, "High-Permittivity (Ba,Sr)TiO_3 Thin Films;" pp. 99–167 in *Handbook of Thin Film Materials*, Vol. 3, Edited by H. S. Nalwa. Academic Press, New York, 2002.

[2]Y. Gao, C. L. Perkins, S. He, P. Alluri, T. Tran, S. Thevuthasan, and M. A. Henderson, "Mechanistic Study of Metal-Organic Chemical Vapor Deposition of (Ba,Sr)TiO_3 Thin Films," *J. Appl. Phys.*, **87** [10] 7430–7 (2000).

[3]S. Y. Lee and T. Y. Tseng, "Electrical and Dielectric Behavior of MgO Doped $Ba_{0.7}Sr_{0.3}TiO_3$ Films on Al_2O_3 Substrate," *Appl. Phys. Lett.*, **80** [10] 1797–9 (2002).

[4]K. P. Jayadevan and T. Y. Tseng, "Composite and Multilayer Ferroelectric Thin Films: Processing, Properties and Applications," *J. Mater. Sci.: Mater. Electron.*, **13** [8] 439–59 (2002).

[5]C. Y. Liu, H. T. Lue, and T. Y. Tseng, "Effects of Nitridation of Silicon and Repeated Spike Heating on the Electrical Properties of $SrTiO_3$ Gate Dielectrics," *Appl. Phys. Lett.*, **81** [23] 4416–8 (2002).

[6]M. S. Tsai, S. C. Sun, and T. Y. Tseng, "Effect of Oxygen to Argon Ratio on Properties of (Ba,Sr)TiO_3 Thin Films Prepared by Radio-Frequency Magnetron Sputtering," *J. Appl. Phys.*, **82** [7] 3482–7 (1997).

[7]S. Safar, R. E. Jones, B. Jiang, B. White, P. Chu, D. Taylor, and S. Gillespie, "Oxygen Vacancy Mobility Determined from Current Measurements in Thin $Ba_{0.5}Sr_{0.5}TiO_3$ Films," *Appl. Phys. Lett.*, **73** [2] 173–7 (1998).

[8]A. Srivastava, D. Kumar, R. K. Singh, H. Venkataraman, and W. R. Eisestadt, "Improvement in Electrical and Dielectric Behavior of (Ba, Sr)TiO_3 Thin Films by Ag Doping," *Phys. Rev. B*, **61** [11] 7305–7 (2000).

[9]J. Assal, B. Hallstedt, and L. J. Gauckler, "Thermodynamic Assessment of the Silver–Oxygen System," *J. Am. Ceram. Soc.*, **80** [12] 3054–6 (1997).

[10]Y. C. Her, Y. C. Lan, W. C. Tsu, and S. Y. Tsai, "Effect of Constituent Phases of Reactively Sputtered AgO_x Film on Recording and Readout Mechanisms of Super-Resolution Near-Field Structure Disk," *J. Appl. Phys.*, **96** [3] 1283–8 (2004).

[11]D. M. Tahan, A. Safari, and L. C. Klein, "Preparation and Characterization of $Ba_xSr_{1-x}TiO_3$ Thin Films by a Sol–Gel Technique," *J. Am. Ceram. Soc.*, **79** [6] 1593–8 (1996).

[12]P. M. Ajayan and L. D. Marks, "Experimental Evidence of Quasi-Melting in Small Particles," *Phys. Rev. Lett.*, **63** [3] 279–82 (1989).

[13]C. Miot, E. Husson, C. Proust, R. Erre, and J. P. Coutures, "X-Ray Photoelectron Spectroscopy Characterization of Barium Titanate Ceramics Prepared by Citric Route. Residual Carbon Study," *J. Mater. Res.*, **12** [9] 2388–92 (1997).

[14]Y. Fujisaki, Y. Shimamoto, and Y. Matsui, "Analysis of Decomposed Layer Appearing on the Surface of Barium Strontium Titanate," *Jpn. J. Appl. Phys. Part 2*, **38** [1A/B] L52–4 (1999).

[15]V. Craciun and R. K. Singh, "Characteristics of the Surface Layer of Barium Strontium Titanate Thin Films Deposited by Laser Ablation," *Appl. Phys. Lett.*, **76** [14] 1932–4 (2000).

[16]F. Amy, A. Wan, A. Kahn, F. J. Walker, and R. A. McKee, "Surface and Interface Chemical Composition of Thin Epitaxial $SrTiO_3$ and $BaTiO_3$ Films: Photoemission Investigation," *J. Appl. Phys.*, **96** [3] 1601–6 (2004).

[17]S. J. Wang and C. K. Ong, "Epitaxial Y-Stabilized ZrO_2 Films on Silicon: Dynamic Growth Process and Interface Structure," *Appl. Phys. Lett.*, **80** [14] 2541–3 (2002).

[18]A. I. Boronin, S. V. Koscheev, K. T. Murzakhmetov, V. I. Avdeev, and G. M. Zhidomirov, "Associative Oxygen Species on the Oxidized Silver Surface Formed Under O_2 Microwave Excitation," *Appl. Surf. Sci.*, **165** [1] 9–14 (1999).

[19]X. Bao, U. Wild, M. Muhler, B. Pettinger, R. Schlögl, and G. Ertl, "Coadsorption of Nitric Oxide and Oxygen on the Ag(110) Surface," *Surf. Sci.*, **425** [2–3] 224–32 (1999).

[20]V. I. Avdeev and G. M. Zhidomirov, "Ethylene and Oxygen Species Adsorbed on a Defect Oxidized Surface Ag(111): Theoretical Analysis by DFT Method," *Surf. Sci.*, **492** [1–2] 137–51 (2001).

[21]D. Y. Zemlyanov, E. Savinova, A. Scheybal, K. Doblhofer, and R. Schlögl, "XPS Observation of OH Groups Incorporated in an Ag(111) Electrode," *Surf. Sci.*, **418** [2] 441–56 (1998).

[22]K. S. Song, S. K. Kang, and S. D. Kim, "Preparation and Characterization of Ag/MnO_x Perovskite Catalysts for CO Oxidation," *Catal. Lett.*, **49** [1–2] 65–8 (1997).

[23]V. R. Choudhary, B. S. Uphade, and S. G. Pataskar, "Low Temperature Complete Combustion of Methane Over Ag-Doped $LaFeO_3$ and $LaFe_{0.5}Co_{0.5}O_3$ Perovskite Oxide Catalysts," *Fuel*, **78** [8] 919–21 (1999).

[24]W. X. Xu, S. Zhu, J. Zhou, X. C. Fu, and X. N. Zhao, "Atomic-Dimensional Film of TiO_{2-x} and its Quantum Size Effect: UV–VIS, XPS, SEM and TEM study," *J. Chem. Soc., Faraday Trans.*, **93** [23] 4187–95 (1997).

[25]M. Bielmann, P. Schwaller, P. Ruffieux, O. Gröning, L. Schlapbach, and P. Gröning, "AgO Investigated by Photoelectron Spectroscopy: Evidence for Mixed Valence," *Phys. Rev. B*, **65** [23] 5431–5 (2002).

[26]D. Peterka, C. Tegenkamp, K. M. Schröder, W. Ernst, and H. Pfnür, "Oxygen Surplus and Oxygen Vacancies on the Surface of Epitaxial MgO Layers Grown on Ag(100)," *Surf. Sci.*, **431** [1–3] 146–55 (1999).

[27]G. I. N. Waterhouse, G. A. Bowmaker, and J. B. Metson, "Interaction of a Polycrystalline Silver Powder with Ozone," *Surf. Inerface Anal.*, **33** [5] 401–9 (2002).

[28]K. P. Jayadevan, N. V. Kumar, R. M. Mallya, and K. T. Jacob, "Use of Metastable, Dissociated and Charged Gas Species in Synthesis: A Low Pressure Analogue of the High Pressure Technique," *J. Mater. Sci.*, **35** [10] 2429–34 (2000).

[29]L. H. Tjeng, M. B. Meinders, J. van Elp, J. Ghijsen, G. A. Sawatzky, and R. L. Johnson, "Electronic Structure of Ag_2O," *Phys. Rev. B*, **41** [5] 3190–9 (1990).

[30]J. H. Pei, C. G. Olson, and R. Manzke, "Surface Core-Level Binding Energy Shifts of InAs," *Chinese J. Phys.*, **26** [2] 90–5 (1988).

[31]S. J. Shih and W. H. Tuan, "Solubility of Silver and Palladium in $BaTiO_3$," *J. Am. Ceram. Soc.*, **87** [3] 401–7 (2004).

[32]T. A. Byrne and D. P. Cann, "Effect of Silver on Barium Titanate as a Function of Stoichiometry," *J. Am. Ceram. Soc.*, **87** [5] 875–80 (2004).

[33]R. D. Shannon, "Revised Effective Ionic Radii and Systematic studies of Interatomic Distances in Halides and Chalcogenides," *Acta Crystallogr.*, **32A**, 751–67 (1972).

[34]B. Kucharczyk and W. Tylus, "Effect of Pd or Ag Additive on the Activity and Stability of Monolithic $LaCoO_3$ Perovskites for Catalytic Combustion of Methane," *Catal. Today*, **90** [1–2] 121–6 (2004).

[35]C. Y. Chen and W. H. Tuan, "Effect of Silver on the Sintering and Grain-Growth Behavior of Barium Titanate," *J. Am. Ceram. Soc.*, **83** [12] 2988–92 (2000).

[36]A. R. Williams and N. D. Lang, "Core-Level Binding Energy Shifts in Metals," *Phys. Rev. Lett.*, **40** [14] 954–7 (1978).

[37]N. Halder, A. D. Sharma, S. K. Khan, A. Sen, and H. S. Maiti, "Effect of Silver Addition on the Dielectric Properties of Barium Titanate Based Low Temperature Processed Capacitors," *Mater. Res. Bull.*, **34** [4] 544–50 (1999).

[38]K. P. Jayadevan, C. Y. Liu, and T. Y. Tseng, "Dielectric Characteristics of Nanocrystalline Ag–$Ba_{0.5}Sr_{0.5}TiO_3$ Composite Thin Films," *Appl. Phys. Lett.*, **87** [2] 1211–3 (2004).

[39]R. Waser and D. M. Smyth, "Defect Chemistry, Conduction, and Breakdown Mechanism of Perovskite-Structure Titanates;" pp. 47–92 in *Ferroelectric Thin Films: Synthesis and Properties*, Edited by C. P. de Araujo, J. F. Scott, and G. W. Taylor. Gordon and Breach Publishers, UK, 1996. □